TISSUE ENGINEERING: Part C
Volume 18, Number 11, 2012

DOI: 10.1089/ten.tec.2012.0119

Methods Article

Rolling the Human Amnion to Engineer Laminated Vascular Tissues

Salma Amensag, M.Sc., and Peter S. McFetridge, Ph.D.

The prevalence of cardiovascular disease and the limited availability of suitable autologous transplant vessels for coronary and peripheral bypass surgeries is a significant clinical problem. A great deal of progress has been made over recent years to develop biodegradable materials with the potential to remodel and regenerate vascular tissues. However, the creation of functional biological scaffolds capable of withstanding vascular stress within a clinically relevant time frame has proved to be a challenging proposition. As an alternative approach, we report the use of a multilaminate rolling approach using the human amnion to generate a tubular construct for blood vessel regeneration. The human amniotic membrane was decellularized by agitation in 0.03% (w/v) sodium dodecyl sulfate to generate an immune compliant material. The adhesion of human umbilical vein endothelial cells (EC) and human vascular smooth muscle cells (SMC) was assessed to determine initial binding and biocompatibility (monocultures). Extended cultures were either assessed as flat membranes, or rolled to form concentric multilayered conduits. Results showed positive EC adhesion and a progressive repopulation by SMC. Functional changes in SMC gene expression and the constructs' bulk mechanical properties were concomitant with vessel remodeling as assessed over a 40-day culture period. A significant advantage with this approach is the ability to rapidly produce a cell-dense construct with an extracellular matrix similar in architecture and composition to natural vessels. The capacity to control physical parameters such as vessel diameter, wall thickness, shape, and length are critical to match vessel compliance and tailor vessel specifications to distinct anatomical locations. As such, this approach opens new avenues in a range of tissue regenerative applications that may have a much wider clinical impact.

Introduction

In the search for biomaterials that improve the regenerative potential of tissue-engineered implants, a number of alternate strategies have been investigated. From a materials perspective, three different approaches have been adopted: the first developing new (or modifying existing) synthetic polymers,[1–3] a second using cell-based technology,[4–7] and a third group using biologically derived materials either as purified compounds or directly as processed *ex vivo* tissues.[8–10] The potential advantage of using complex biological bioscaffolds is that critical cues driven by matrix-associated functional groups will enhance tissue regeneration. Small-diameter blood vessel grafts (< 6 mm inside diameter) are extremely sensitive to occlusive failure, particularly by thrombotic and hyperplastic activity, and as such, materials that speed regeneration and promote a more quiescent phenotype may prove to be more successful.

The human amniotic membrane (hAM) is an abundant birthing tissue that, due to its unique structure, composition, and neonatal derivation, has been clinically used in applications such as ocular, skin, cartilage, and peripheral nerve regeneration with promising results.[11–17] However, all these applications have used the hAM as an acellular material, without taking advantage of the material's capacity to be seeded or used as a layered construct to speed and potentially enhance tissue regeneration. The hAM presents a number of desirable characteristics (advantageous for blood vessel regeneration and a wide range of tissue-engineering applications), including biocompatibility, biostability, noninflammatory, nontoxic, noncarcinogenic, nonimmunogenic,[17] vasoactivity, thromboresistance,[18] ability to remodel,[16] infection resistance, suture-holding capacity,[19] and its wide availability.

A significant hurdle with many *ex vivo*-derived materials is the inability to produce a cell-dense construct quickly, as seeded cells need to migrate through the entire scaffold, which can be time consuming and further promote the loss of functional phenotypes. Previous groups have developed cell-sheet-based rolling technologies for blood vessel development, without the use of additional three-dimensional (3D) scaffold structures.[4–7] While this approach has shown positive results, the regenerative process can be lengthy and

J. Crayton Pruitt Family Department of Biomedical Engineering, University of Florida, Gainesville, Florida.

maybe problematic for procedures requiring rapid delivery. In order to develop engineered tissues in restricted clinical time lines, a cell-dense construct described here is a new approach that combines the use of *ex vivo* scaffolds in concert with cell-sheet-based technology. This approach consists of creating a multilayered structure (cells/human human amniotic membrane scaffold [hAMS]/cells/hAMS etc.), where the hAMS form multiple layers "sandwiching" cells to form a cell-dense material. Thus, layers can be in close proximity to promote cell-cell communication (between layers and possibly across the construct) as remodeling progresses. This is an important requirement that recapitulates the functionality of the complex vascular wall.

The primary objective of these investigations was to adapt the hAM from a flat sheet membrane into a laminated, tubular bioscaffold using cells to produce *de novo* blood vessels that have the potential to be implanted during early regenerative processes. The multiple layers ($\sim$50 μm thick) were hypothesized to more closely resemble the natural 3D vascular environment and promote vascular remodeling. hAM sections were decellularized with 0.03% sodium dodecyl sulfate (SDS),[20] and then reseeded with either endothelial cells (EC) or smooth muscle cells (SMC). Cell function was assessed to determine variations in cell adhesion, cell density, metabolic activity, and changes in the material's biomechanical properties over 40 days of cell culture.

The utility of this new laminate approach to process the hAMS and form a tubular structure is particularly promising for vascular bypass surgeries where the clinical time frame from patient diagnosis to treatment can be extremely short. As such, the capacity to produce vessels in physiologically relevant diameters and thicknesses that also meet specific demands for biological and mechanical performance criteria is crucial.

Materials and Methods

Procurement and isolation of the hAM

Over the experimental time course, $\sim$20 full-term human placentas were collected from the Woman's Delivery Center at the Norman Regional Hospital, Norman, OK, and the Shands Gainesville hospital in Florida, the United States.

Bioscaffold preparation

Immediately on collection, hAM samples were manually isolated from the chorionic membrane and rinsed twice in deionized water. hAM sections were then devitalized by two cycles of freezing (2 h at −86°C) and thawing (15 min at 37°C). The samples were immersed in 0.03% (w/v) SDS and agitated at 100 rpm on an orbital shaker plate for 24 h at 25°C.[20,21] Successive rinses in deionized water of the samples (5, 15, 40 min, 1, and 6 h) preceded an overnight incubation at 37°C in 50 U/mL in a desoxyribonuclease (DNase) solution (Sigma, St. Louis). After three rinses in deionized water, the samples were sterilized for 2 h in a 0.01% (vol/vol) peracetic and ethanol (2% vol/vol) solution (Fluka). The samples were then pH balanced in phosphate-buffered saline (PBS) with successive rinses as just described. The total processing time from placental collection to the final sterile scaffold was $\sim$72 h, at which point the scaffolds were incubated in standard SMC cell culture media overnight at 37°C and immediately used for construct development.

Scaffolds were independently assessed as "flat" or "rolled" constructs. Flat constructs were dissected from decellularized hAM into 15 mm-diameter disks in order to fit standard six-well tissue culture plates (Corning). Scaffolds prepared for rolling were cut from decellularized hAM sheets into $13 \times 9\,cm^2$ rectangular sections. These sections were seeded as flat sheets and cultured for 10 days before rolling into the tubular structure. The rolling procedure oriented the basement membrane upper most and was rolled five times around a 4.2 mm-diameter glass rod, as shown in Figures 1A–D and 2A. Seeded flat sections were assessed at days 0, 2, 4, 6, 10, 20, and 40, and rolled constructs (being rolled at day 10) were assessed on days 20, 30, and 40.

Cell culture

Human SMC purchased from the ATCC (batch 2654) were expanded until passage 9. Human umbilical vein endothelial cells were enzymatically isolated from the human umbilical vein and expanded using Vasculife VEGF cell culture media (Lifeline Cell Technology) until passage 4. The cells were maintained in Dulbecco's Modified Eagle's Medium (DMEM; Invitrogen), supplemented with 1% penicillin-streptomycin (Gibco Life technologies), and 10% of fetal serum complex (FetalPlex; Genimini Bio-Products), and replenished every 3 days. The cells were cultured in a 5% CO_2 humidified incubator at 37°C. Subconfluent cells were enzymatically detached from the culture flasks using Trypsin (Invitrogen). Under sterile conditions, cells at a subconfluent density (600 cells/mm^2) were seeded onto the stromal surface of hAMS sections.

Cell adhesion

Independent monocultures of SMC and EC were seeded onto flat hAM scaffolds and stained with 4′-6-diamidino-2-phenylindole (DAPI stain; Invitrogen) at a 300 nM concentration 2 h after seeding to identify cell nuclei. A Carl Zeiss Axio Imager M2 Epifluorescent microscope) was calibrated to image 400×325 μm ($0.13\,cm^2$), using the 20× objective.

SMC proliferation and metabolic activity

At each time point, flat and rolled hAMS sections were digested using the proteolytic enzyme Papain (Spectrum) at a 125 μg/mL concentration for 24 h at 60°C. Degraded samples were then centrifuged, and the supernatant was analyzed to quantify the amount of DNA per sample using the Quanti-iT PicoGreen assay as per manufacturer's instructions (Invitrogen). SMC metabolic activity was assessed using the Alamar Blue assay kit (Invitrogen). Absorbance was measured at 570 and 600 nm. The calculated reduction of Alamar Blue was used as an indicator of cell metabolic activity that was correlated with cell density to give the metabolic activity per cell against a calibration curve of the same cell lineage.

Glycosaminoglycan analysis

Samples were digested in a solution containing 125 μg/mL of papain for 24 h at 60°C. Glycosaminoglycan (GAG) content was assessed using dimethylmethylene blue (Sigma

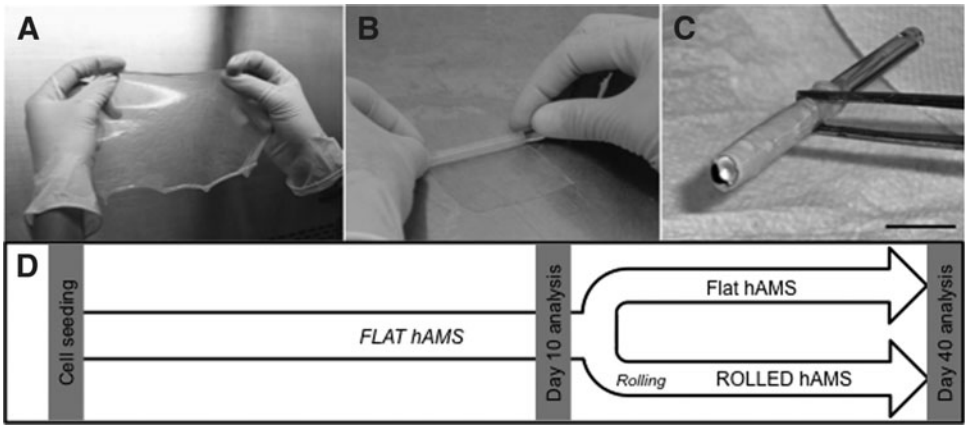

FIG. 1. hAM preparation and rolling procedure. The hAM **(A)** was first decellularized, then under sterile conditions cut to $13 \times 9\,cm^2$ sections. SMC were seeded at a concentration of 600 cells/mm^2 and cultured as flat sheets for 10 days before rolling **(B)**. After a further 10 days of culture, the hAMS was rolled five times around a glass mandrel **(C)**. A pictorial overview of construct seeding, rolling, and terminal analysis **(D)**. Scale bar in **(C)** = 1 cm. hAM, human amniotic membrane; hAMS, human amniotic membrane scaffold; SMC, smooth muscle cells.

Aldrich) and calibrated using the chondroitin sulfate as a standard.[20,22,23]

Tissue biomechanics

Tensile properties were assessed using an Instron uniaxial testing rig (Model 5542, with Version 2.14 software; Instron). Tissue disks were rinsed in PBS and cut to an oblong shape maintaining a 5:1 (length: width) ratio. Tissue strips were then loaded between two vertically parallel clamps with cyanoacrylate glue used to prevent slippage, and progressively tensioned to reach a preloaded of ~0.1 N. Samples were then tensioned until failure at a constant rate of 5 mm/min. Load and displacement values were recorded to calculate the stress/strain relationship. Strain values were obtained by normalizing sample deformation $(L_F\text{-}L_I)$ to initial length L_I, where L_F, is the extension at failure using the equation. $\varepsilon = \frac{(L_F - L_I)}{L_I}$ Stress values were calculated by dividing load F to the initial cross-sectional area values of each sample using $\sigma = \frac{F}{(tw)}$. where t is the thickness of the sample, and w is its width. Based on our observations and published data, the thickness of a single hAM layer was estimated to be 50 μm.[24,25] To assess the rolled constructs, the same preload and testing parameters were used on dissected 5 mm-wide ringlets attached to the test rig using stainless L-shaped hooks. While being less accurate than true stress, engineering stress was used to approximate the materials' bulk properties. The engineering stress values for ringlets was calculated using $\sigma = \frac{F}{(2tw)}$ where $2tw$ is the cross-sectional area of the ringlet. The elastic modulus (EM) corresponds to the stress/strain (σ/ε),[26] which is defined as force/unit area. EM was assessed from 0.01 MPa (80 mmHg) to a maximum of 0.02 MPa (120 mmHg) corresponding to a low-strain region that reflects physiologic behavior (physiologic range).[27,28] The stress of a thin-wall elastic tube corresponds to $Pd/2t$, where P is the transmural pressure, d is the diameter, and t is the thickness. As such, the construct compliance in the physiological range (80 to 120 mmHg) $(\Delta d/d)/P$ was calculated in

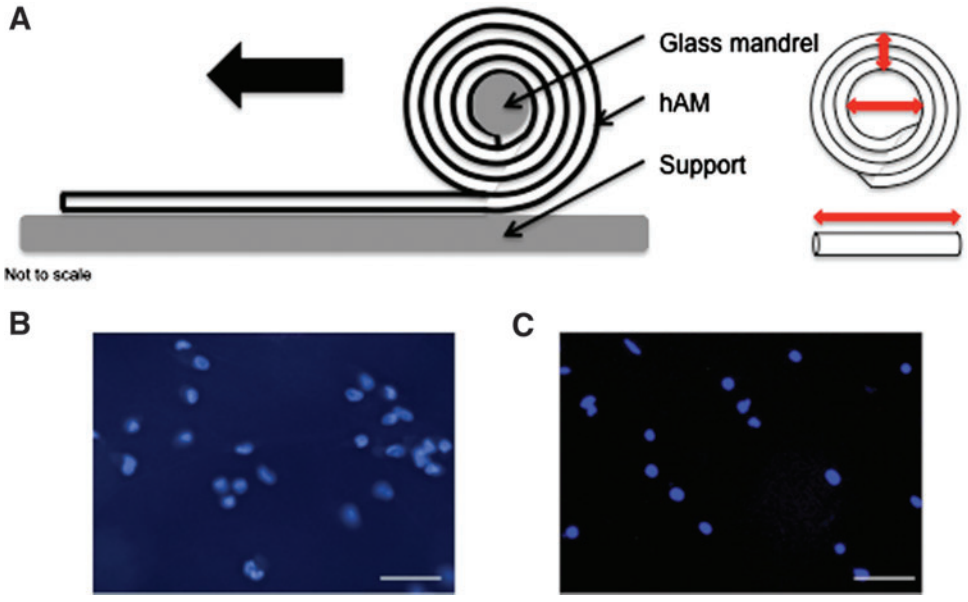

FIG. 2. Schematic of the rolling process and initial adhesion of EC and SMC monocultures. **(A)** Schematic on the right shows the rolling process with the layered structure, with the left image showing tunable geometries in scaffold size (lumen diameter, length, and number of membrane revolutions). Initial adhesion of EC **(B)** and SMC **(C)** monocultures was assessed 2 h after seeding using the fluorescent nuclear stain DAPI. Scale bar = 50 μm. EC, endothelial cells. Color images available online at www.liebertpub.com/tec

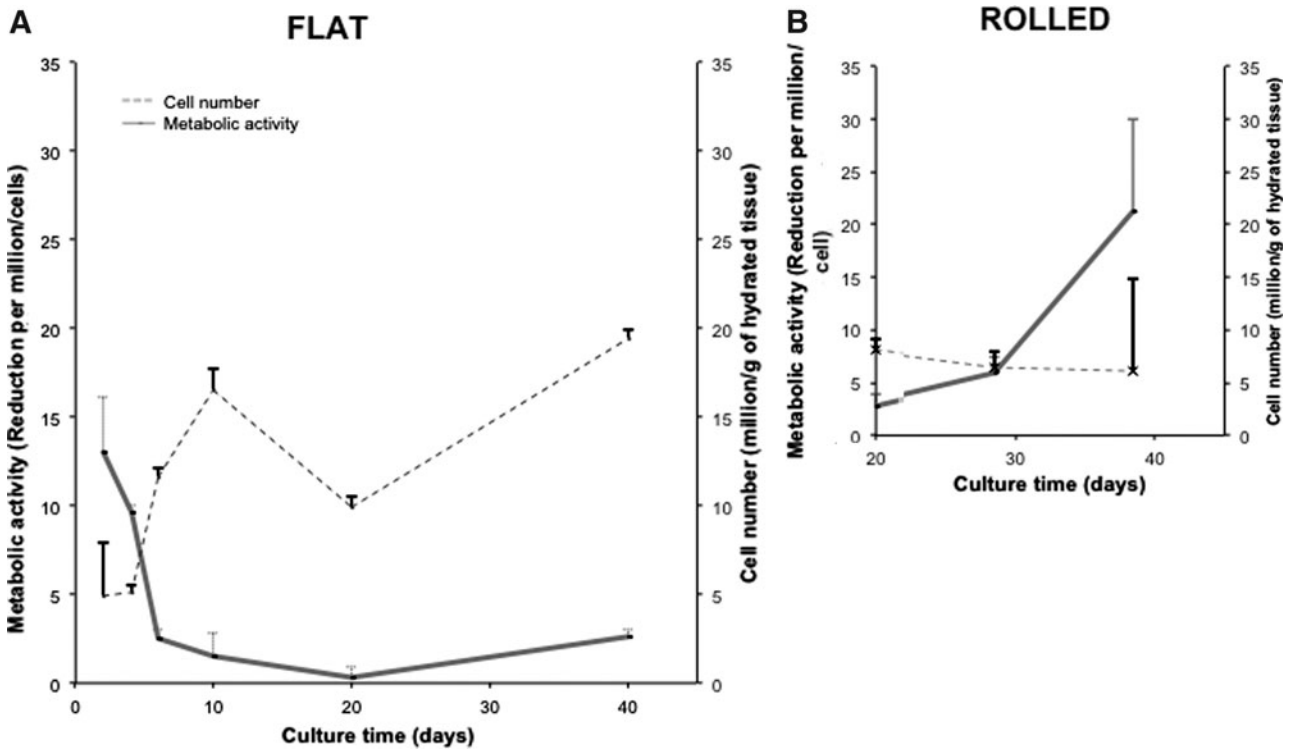

FIG. 3. SMC metabolic activity and cell density when cultured on and within the hAMS. Quantitative assessment of cell metabolic activity and cell proliferation for flat sheets **(A)** and rolled constructs **(B)**. On flat constructs, the cells displayed an increasing cell population, with a decreasing cell metabolic activity. Conversely, cells within rolled constructs (after day 10) showed no statistical change in cell density to day 40; however, a significant increase in metabolic activity was noted ($n=3$).

%/mmHg as $d/(EM2t)$.[26] The rupture strength corresponds to the maximum stress at sample rupture.

Scanning electron microscopy

Samples were fixed in 2.5% glutaraldehyde (Sigma) for 4 h and then washed thrice in PBS for 5 min. This was followed by a treatment of 1% osmium tetroxide (Acros Organics N.V.) solution for 2 h.[24,29] The samples were then progressively dehydrated in a series of graded ethanol solutions, and then CO_2 critically point dried (Autosamdri-814; Tousimis). The samples were then gold sputtered (Hummer IV) and analyzed using a JEOL LSM-880 scanning electron microscopy (SEM) at 10 kV.

RNA extraction and quantitative reverse transcription-polymerase chain reaction

Total RNA was isolated from tissues using the miVarna isolation kit (Ambion). Thereafter, cDNA was synthesized from 2 μg of the total RNA using SuperScript VILO cDNA Synthesis Kit (Invitrogen). Primers for semi-quantitative reverse transcription–polymerase chain reaction (RT-PCR) were purchased from Integrated DNA Technologies (IDT). Primer sequences used in this study were as follows: human SM-α actin: forward primer: 5′-CATCACCAACTGGGACGA-3′, reverse primer: 5′-GGTGGGATGCTCTTCAGG-3′; *SM22:* forward primer: 5′-GG CAGCTTGGCAGTGACC-3′, reverse primer: 5′-TGGCTCTCT GTGAATTCCCTCT-3′; *COL1A1*: forward primer: 5′-ATG TGGCCATCCAGCTGAC-3′, reverse primer: 5′-TCTTGCAG TGGTAGGTGATGTTCT-3′. RT-PCR reactions were run using a BioRad CFX96 and CFX384 Real-Time Systems with glyceraldehyde-3-phosphate dehydrogenase used as an internal control. The first cycle was defined at 95°C for 10 min, followed by 40 cycles of denaturing at 95°C for 15 s, annealing/extension at 60°C for 60 s. The amount of DNA immunoprecipitated was determined using quantitative real-time PCR using Power SYBR green PCR master mix (SA Biosciences). Relative mRNA levels were evaluated by BioRad CFX Manager Software (BioRad) and calculated using the $2^{-\Delta\Delta Ct}$ method normalized to the expression level in basal culture conditions, and expressed as the fold difference relative to the SMC seeded onto T75 flasks (served as controls).

Histology

Frozen sections (5 μm) were cut using a cryostat (Thermoscientific Microm HM 550), stained with Hematoxylin and Eosin as per standard protocols, and then imaged using a Carl Zeiss Axio Imager M2 Epifluorescent microscope).

Bioreactor assembly

Dual perfusion vascular bioreactors were used with a length of 100 mm and an internal diameter of 13 mm, as previously described.[27,30] Bioreactors were connected in series (x3) with independent lumen and ablumen flow circuits. Peristaltic pumps (Cole Parmer L/S digital Standard Drive, model EW-07551-10) were used to perfuse respective medias at a flow rate of 60 mL/min (lumen) and 30 mL/min (ablumen) at a pulse frequency of 1 Hz. Nylon thread (0.32 mm) was wrapped around each construct to prevent initial

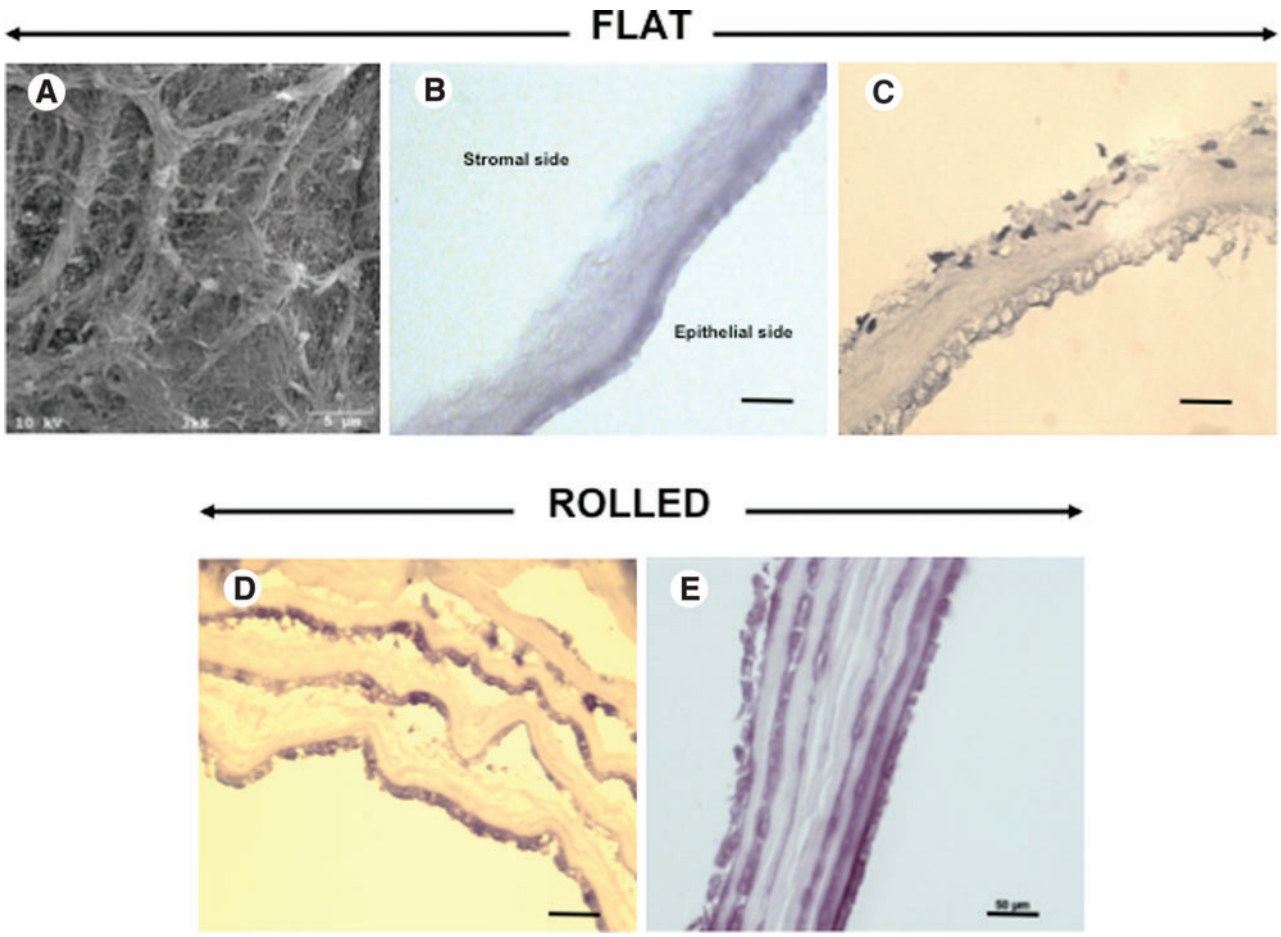

FIG. 4. SEM and histological image analysis. SEM of the hAMS stromal surface after sodium dodecyl sulfate decellularization **(A)** displayed fibers with a random orientation and no observable cellular debris. Histological sections of the decellularized hAMS show the stromal surface to have a compact fiber structure, with a relatively thick stromal layer compared with the thinner and more compact basement membrane **(B)**. Day 10 after cell seeding, cell migration into the stromal layer was observed **(C)**. The multilayered construct at day 20 **(D)**, and at day 40 **(E)** showing areas of higher cell concentration with a more compact and remodeled ECM compared with the native ECM. Scale bar = 50 μm for histological images and 5 μm for SEM images. SEM. Color images available online at www.liebertpub.com/tec

unwinding. Systems were maintained at 5% CO_2 and 37°C. Culture medium was 100% replenished every 3 days.

Statistical analysis

Unless otherwise stated, all data are presented as mean values ± standard deviation from at least three independent experiments ($n = 3$). Statistical analysis was performed using the two-way analysis of variance method with significant differences corresponding to a $p < 0.01$ (confidence level ≥ 99%).

Results

Scaffold rolling, cell adhesion, and early regenerative events

As an assessment of initial cell adhesion, EC and SMC were seeded on independent scaffolds (flat membranes) at a density of 1×10^4 cells/mg wet tissue (corresponding approximately to 600 cells/mm^2). As discrete cultures, both EC and SMC were shown to adhere to the stromal surface, as seen by localization of the nuclear binding dye DAPI (see Figure 2B and C, respectively). Extended monocultures of SMC show cells as proliferating with a quantitative increase in density reaching 16.5 million of cells/g of hydrated tissue over the first 10 days (Fig. 3A), to 19.5 million cells/g by day 40. As the cell population increased, a progressive decline in metabolic activity was noted, showing a fivefold reduction from day 2 to day 40. The rolled hAMS (Fig. 3B) from day 20 through day 40 displayed a different trend compared with the flat constructs showing a rising metabolic activity in association with a slight decrease in cell density.

Similar to the stromal surface of the native hAM, an SEM analysis of decellularized scaffolds shows the surface structure and morphology as having no specific fiber orientation after processing steps. The overall structure of ECM was shown to be compact with a relatively compressed or matted fibrillar structure (Fig. 4A, B). Histology images show the cells to be localized between adjacent hAM layers, as well as having migrated into the existing matrix by day 10 (Fig. 4C).The cells were noted between the concentric layers with observable remodeling activity that appears to be binding the adjacent layers together (Fig. 4D, E).

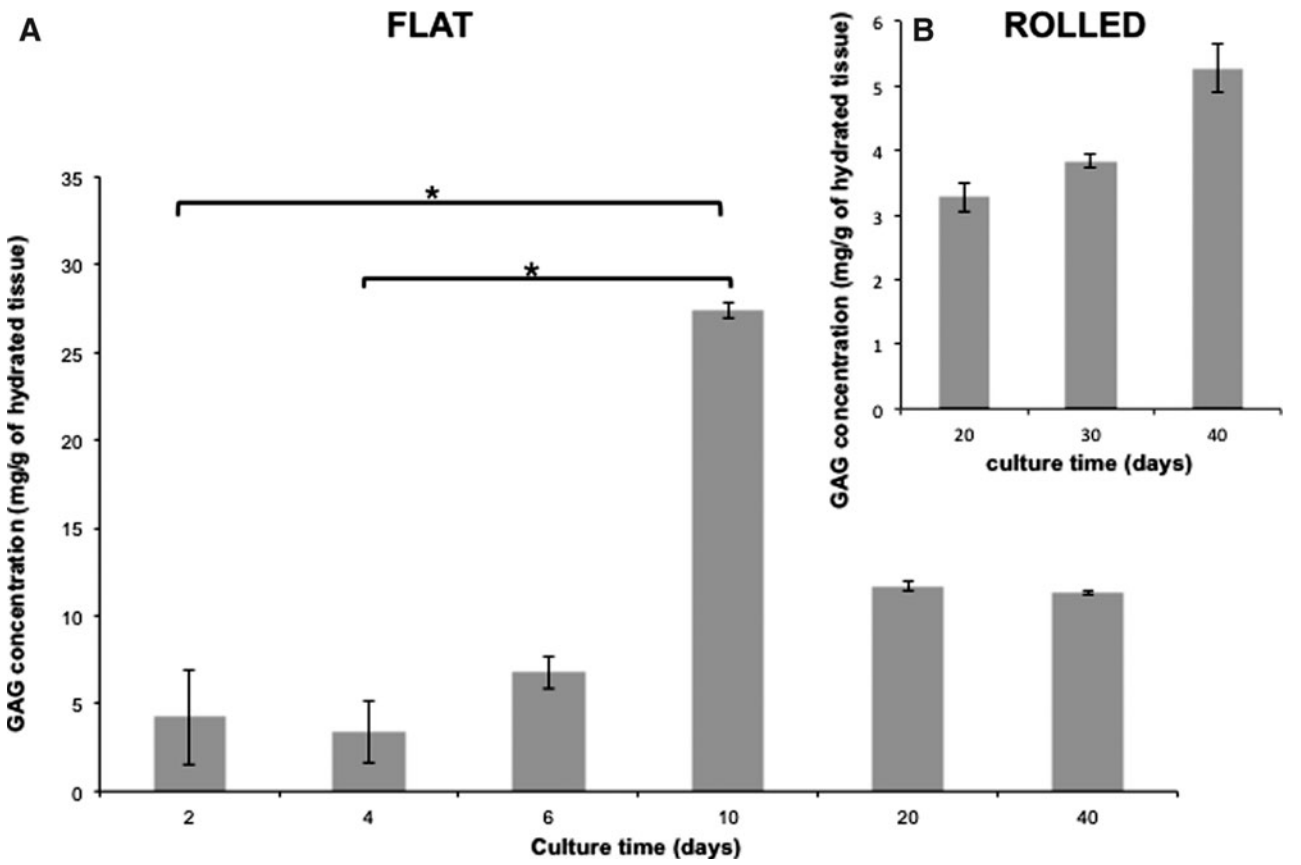

FIG. 5. Changes in GAG concentration. GAG concentrations increased over 10 days of cell culture with the flat hAMS **(A)**, stabilizing at day 20 to 10 mg/g of hydrated tissue. A progressive increase of GAG concentration was measured with the rolled hAMS **(B)** from day 20 to 40 ($n=9$). ($n=5$). *$p<0.01$. GAG, glycosaminoglycan.

The production of GAG by cells seeded on the bioscaffold was quantified in order to further assess the early remodeling events occurring within the hAMS. Following a similar trend to cell density, the GAG concentrations on flat constructs increased until day 10 (27.4 mg/g), and then reduced to a stable concentration of 11 mg/g of hydrated tissue (Fig. 5A) until day 40. In accordance with the noted increased metabolic activity and cell density, the GAG concentration on rolled constructs progressively increased from 3.3. to 5.2 mg/g of hydrated tissue from day 20 to day 40 (Fig. 5B).

The expression of SMC phenotypic markers α-actin and SM22, as well as collagen was assessed on flat hAMS at day 10, and on rolled hAMS at day 20 and 40 postseeding (corresponding to 10 and 20 days after the rolling process); see Figure 6. Cells cultured on standard tissue culture plastic served as controls. Alpha-actin was expressed at each time point with a 13-fold higher expression at day 40 compared with the controls. At days 10 and 20, SM22 gene expression levels had similar values to controls but at day 40, an 11.2-fold increase in expression was shown. Collagen I expression decreased from a peak of 2.8-fold over controls at day 10 to the same level as controls by day 40.

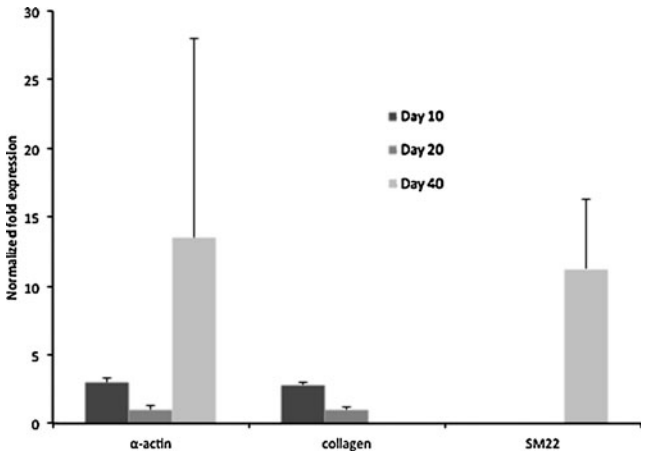

FIG. 6. Reverse transcription–polymerase chain reaction of rolled hAMS at day 10, 20, and 40. Variation in gene expression profiles of collagen and SMC phenotype markers α-actin and SM22 by SMC was assessed. Data were calculated using the $2^{-\Delta\Delta Ct}$ method normalized to SMC expression levels under basal culture conditions (controls), and expressed as the fold differences. At each time point, α-actin was expressed at higher levels than controls, reaching an 11-fold increase by day 40. SM22 was expressed with higher values than controls at day 40 only. Collagen expression decreased from 2.8-fold at day 20 to same values as those of the controls at day 40.

Mechanical properties and dynamic culture

Static culture. Typical of biological soft tissues, both flat and rolled constructs displayed a biphasic force/strain response. The EM was assessed over the physiological pressure

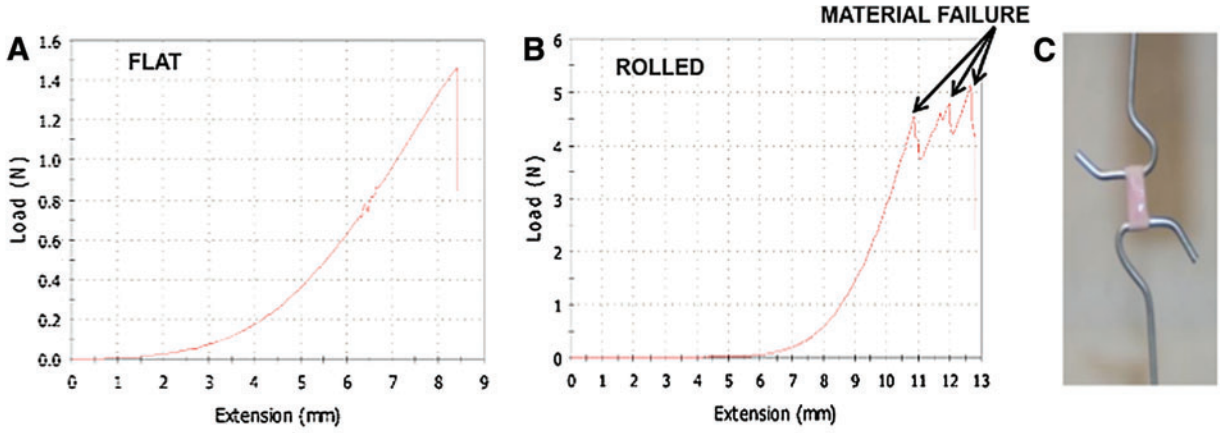

D

	FLAT hAM									ROLLED hAM		
	Control	Day 2	Day 4	Day 6	Day 8	Day 10	Day 20	Day 30	Day 40	Day 20	Day 30	Day 40
Physiological modulus (MPa)	0.34 ±0.2	0.46 ±0.1	0.40 ±0.1	0.41 ±0.2	0.25 ±0.1	0.22 ±0.1	0.2 5±0.1	0.01 ±0.01	0.0 4±0.1	0.08 ±0.01	0.03 ±0.001	0.04 ±0.001
Rupture strength (MPa)	2.35 ±0.7	1.35 ±0.1	1.39 ±0.3	1.89 ±0.4	1.17 ±0.6	1.46 ±0.3	2.36 ±0.5	0.40 ±0.4	0.77 ±0.4	2.120 ±0.2	2.14 ±1.1	1.38 ±0.6

FIG. 7. Tensile properties of the hAMS. Representative plots showing stress-strain relationships for flat **(A)** and rolled **(B)** hAMS. **(C)** details the ringlet test method to assess tensile properties. Single breaking points were observed on flat hAMS **(A),** whereas three breaking points were noted on the five times rolled hAMS. The rupture strength of the laminated hAMS was twice higher at 1.38 MPa compared with single layers of hAMS (0.77 MPa). **(D)** shows tabulated data of the constructs elastic modulus (over the physiological range: 80–120 mmHg) and rupture strength for both flat and rolled constructs. Color images available online at www.liebertpub.com/tec

range (80/120 mmHg).[28,31,32] The constructs increased in mechanical stiffness (EM) as load values increased, resulting in a single failure point with the single layer of hAM (Fig. 7A), while the rolled constructs displayed multiple failure points associated with the fracture of each discrete layer, (Fig. 7B). Figure 7C shows the multilayered scaffold as a 5 mm ringlet (axial) and mounted into the tensile testing rig. The EM (over the physiological range: 80/120 mmHg) and rupture strength displayed a progressive decrease over time, reaching 0.04 and 1.38 MPa, respectively, at day 40, Figure 7D.

Dynamic culture. Figure 8A displays a schematic diagram of the perfusion circuit, with dual flow systems to isolate lumen and ablumenal circuits. A histological assessment of the dynamically stimulated constructs shows the laminate structure to be bound tightly together, forming a uniform tubular construct; see Figure 8B. Construct compliance, EM, and rupture strength relative to human carotid arteries are shown in Figure 8C. The load/extension profile shows three distinct failure points, similar to the profile under static conditions, see Figure 8D.

Discussion

One of the primary challenges in reengineering organs and tissues *in vitro* is the choice of bioscaffold used to direct regenerative events to form biologically and mechanically responsive tissues. The hAM is an abundant birthing tissue that, due to its unique structure, composition, and neonatal derivation, has had promising results when used in a number of tissue repair applications.[11–17,33] Based on these clinical successes and a novel approach that takes advantage of the hAM's unique properties, we have developed a concentric rolling approach that aims at rapidly forming cell-dense and mechanically stable tissue-engineered blood vessels.

Our goal was to evaluate the early remodeling events *in vitro* to estimate the clinical potential of the constructs. Due to the restricted time scale associated with bypass surgeries, the capacity to implant constructs during early remodeling phases would allow the later stages of tissue regeneration to occur *in vivo* where vascular tone, vasa vasorum, and so on are fully developed after the operative event. With this technique, cells seeded on sheets of the processed membrane were rolled around a mandrel to form a tubular construct with concentric layers of cells between each amnion layer. This is a novel approach that allows the generation of a cell-dense material which can be manufactured into different diameters and shapes to suit specific applications, and done so in a timely fashion that may meet surgical requirements. This approach is particularly promising in the vascular area due to the range of diameters, wall thicknesses, and lengths that can be generated for different clinical procedures. Further, the ability to modulate the number of layers gives a degree of control over the bioscaffolds mechanical properties, allowing not only matching tensile properties with a controllable diameter, but also matching compliance values.

Decellularization aims at effectively removing immunogenic cellular material while allowing the bioscaffold to

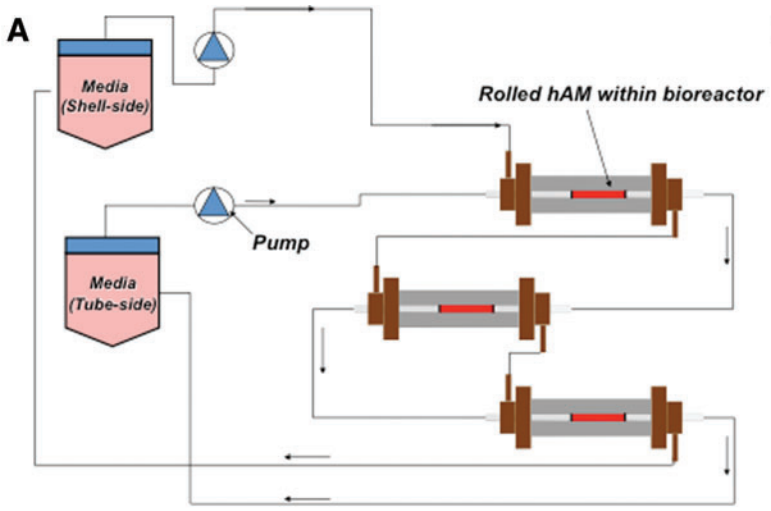

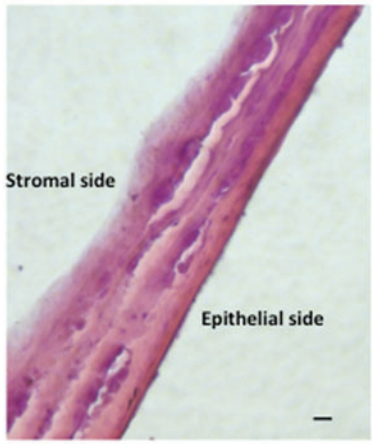

C

	Rupture strength* (MPa)	Elastic modulus* (MPa)	Mean compliance# (%/mmHg)
hAMS (n=5)	1.87	1.17	0.079
Human carotid arteries	2.65 [37]	0.039 [38]	0.158 [39]

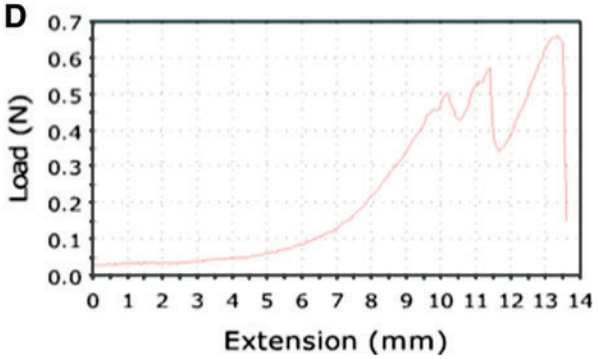

FIG. 8. Dynamic culture and comparative mechanics. A schematic of the dynamic culture systems process flow **(A)**. Two peristaltic pumps drove the respective solutions media and phosphate buffered saline through the albumen and lumen flow circuits at a constant flow rate of 30 and 60 mL/min, respectively. Constructs cultured under perfusion conditions displayed a compact structure at day 40 **(B)**. Rupture strength, elastic modulus, and mean compliance values are compared with native human carotid arteries values **(C)**, #refers to theoretical calculated values. A representative load–extension profile of the rolled construct illustrates multiple failure peaks associated with each construct layer **(D)**. Scale bar in **(B)** = 20 μm. *refers to measured values. Color images available online at www.liebertpub.com/tec

retain a degree of its biological activity and mechanical integrity as a function of the existing ECM. A wide range of methods specific for hAM decellularization have been described, including treatment with the ionic surfactant SDS as used in these investigations.[14,20,21,34–36] SEM and histology data confirm previous findings,[20,21] that SDS decellularization was efficient at removing whole cells, with images showing the ECM to be largely free of cellular remnants.

DAPI images confirmed EC and SMC adherence on the stromal surface of the hAMS 2 h postseeding. An assessment of SMC growth and metabolic activity confirmed proliferation within the scaffold. Interestingly, while the overall metabolic activity increased as a function of increased cell density, on a per-cell basis, metabolic activity decreased as cell density increased. This was hypothesized to be due to an early adaptation time where cells rapidly modify their immediate location with increased ECM synthesis, as indicated with increasing GAG concentrations, and may account for a degree of increased metabolic activity. By contrast, cells within the rolled hAMS maintained a stable cell density until day 40 but displayed an increasing metabolic activity. Overall, these data indicate a capacity of SMC to migrate, proliferate, and secrete GAGs when cultured with the hAMS in either flat or rolled orientations. The reduction in cell density during the transition from flat to rolled constructs was the result of the rolling process where the surface that cells were seeded on developed a gel-like ECM which was displaced as the scaffold was rolled (slightly compressed). This caused portions of this new layer (with cells) to be lost.

The SMC phenotype was assessed by quantifying the expression of SMC-specific markers α-actin, SM22, and the ECM gene collagen type I at day 10 (flat constructs), day 20, and 40 (rolled constructs). Results show that cells expressed these differentiation markers, although significant variations were seen in expression levels. At each time point, α-actin was expressed at higher levels than control samples with SM22 that were only up-regulated at day 40. By day 40, the cells cultured on rolled constructs displayed a high metabolic activity concurrent with a contractile phenotype, as shown by the up-regulation of SM22. The combination of increased metabolic activity in concert with stable cell density and increased contractile function indicates that these remodeling processes are conditional on specific micro-environmental conditions that change overtime.

From a mechanical perspective, engineered blood vessels aim at mimicking the mechanical properties of natural

vessels. In order to reproduce the physiological environment, rolled constructs were mounted into a perfusion circuit to mechanically stimulate cells, and results were compared with the traditional static culture. The EM was assessed over the physiological pressure range (80/120 mmHg),[28,31,32] which is a key mechanical parameter associated with graft compliance. The maximum stress experienced by constructs cultured under dynamic conditions was lower than statically cultured samples. We hypothesize that this is due to the lack of controlled physiological pressure applied to the dynamic system that would otherwise direct cells to remodel the scaffold with a more defined fiber alignment. Given that remodeling is a controlled process that balances catabolic and anabolic activity, further investigations that assess mechanical changes over time in concert with longer culture periods will further our understanding of these processes.

The importance of matching mechanical properties has become evident as our understanding of cell function and material relationships progress. The hAM's rupture strength and EM were compared with human carotid arteries, as detailed by Yokota *et al.* 2009 (see Fig. 8D)[38] showing values in the same order of magnitude for both rupture strength and EM. At day 40, the mean compliance of constructs cultured under static conditions was the same order of magnitude as dynamically cultured hAMS, and comparable to native carotid vessels.

While the structural changes that occur as a function of rolling are obvious and the material properties remain similar, the cellular microenvironment significantly changed when rolled. The dominant effects will either be driven by mass transfer limitations that may inhibit cell function due to nutrient deprivation, or may promote specific cellular phenotypes. Although EC have been successfully cultured on the basement membrane, further investigations under modified co-culture conditions with EC on the lumen with the SMC on adjacent layers to mimic physiological conditions may offer new perspectives on vessel regeneration and remodeling. While the long-term response and *in vivo* validation are still required, this approach shows the utility of the rolling technique to generate a construct with tunable mechanical properties.

These investigations are the first that introduce a novel concentric rolling technique using the hAM as an alternative strategy to develop cell-dense vascular bioscaffolds. Results support the potential of using the hAM as a bioscaffold for the engineering and reconstruction of damaged or diseased blood vessels. This approach is important, as it offers the potential of the construct to be implanted early to complete remodeling *in vivo,* or to be fully developed *in vitro*. Multilaminate vessels can be manufactured with different diameters and wall thicknesses with the possibility of making more complex structures such as vessel bifurcations. In addition, this approach may also serve as an effective *in vitro* model system to study vascular disease and regeneration.

Acknowledgments

This work was supported in part by the National Institutes of Health [R01-HL088207].

The authors would also like to acknowledge the Shand's Hospital (Gainesville, FL) for providing the hAMs used in this study under the University of Florida Institutional Review Board approval certification no. 64–2010.

Disclosure Statement

No competing financial interests exist.

References

1. Puskas, J.E., and Chen, Y. Biomedical application of commercial polymers and novel polyisobutylene-based thermoplastic elastomers for soft tissue replacement. Biomacromolecules **5,** 1141, 2004.
2. Madigan, N.N., McMahon, S., O'Brien, T., Yaszemski, M.J., and Windebank, A.J. Current tissue engineering and novel therapeutic approaches to axonal regeneration following spinal cord injury using polymer scaffolds. Respir Physiol Neurobiol **169,** 183, 2009.
3. Gunatillake, P., Mayadunne, R., and Adhikari, R. Recent developments in biodegradable synthetic polymers. Biotechnol Annu Rev **12,** 301, 2006.
4. L'Heureux, N., Dusserre, N., Konig, G., Victor, B., Keire, P., Wight, T.N., Chronos, N.A., Kyles, A.E., Gregory, C.R., Hoyt, G., Robbins, R.C., and McAllister, T.N. Human tissue-engineered blood vessels for adult arterial revascularization. Nat Med **12,** 361, 2006.
5. L'Heureux, N., Dusserre, N., Marini, A., Garrido, S., de la Fuente, L., and McAllister, T. Technology insight: the evolution of tissue-engineered vascular grafts—from research to clinical practice. Nat Clin Pract Cardiovasc Med **4,** 389, 2007.
6. L'Heureux, N., Germain, L., Labbe, R., and Auger, F.A. *In vitro* construction of a human blood vessel from cultured vascular cells: a morphologic study. J Vasc Surg **17,** 499, 1993.
7. L'Heureux, N., Paquet, S., Labbe, R., Germain, L., and Auger, F.A. A completely biological tissue-engineered human blood vessel. FASEB J **12,** 47, 1998.
8. Dutta, R.C., and Dutta, A.K. Cell-interactive 3D-scaffold; advances and applications. Biotechnol Adv **27,** 334, 2009.
9. Montoya, C.V., and McFetridge, P.S. Preparation of *ex vivo*-based biomaterials using convective flow decellularization. Tissue Eng Part C Methods **15,** 191, 2009.
10. McFetridge, P.S., Bodamyali, T., Horrocks, M., and Chaudhuri, J.B. Endothelial and smooth muscle cell seeding onto processed *ex vivo* arterial scaffolds using 3D vascular bioreactors. ASAIO J **50,** 591, 2004.
11. Kheirkhah, A., Johnson, D.A., Paranjpe, D.R., Raju, V.K., Casas, V., and Tseng, S.C. Temporary sutureless amniotic membrane patch for acute alkaline burns. Arch Ophthalmol **126,** 1059, 2008.
12. Maharajan, V.S., Shanmuganathan, V., Currie, A., Hopkinson, A., Powell-Richards, A., and Dua, H.S. Amniotic membrane transplantation for ocular surface reconstruction: indications and outcomes. Clin Exp Ophthalmol **35,** 140, 2007.
13. Tamhane, A., Vajpayee, R.B., Biswas, N.R., Pandey, R.M., Sharma, N., Titiyal, J.S., and Tandon, R. Evaluation of amniotic membrane transplantation as an adjunct to medical therapy as compared with medical therapy alone in acute ocular burns. Ophthalmology **112,** 1963, 2005.
14. Jin, C.Z., Park, S.R., Choi, B.H., Lee, K.Y., Kang, C.K., and Min, B.H. Human amniotic membrane as a delivery matrix for articular cartilage repair. Tissue Eng **13,** 693, 2007.
15. Mligiliche, N., Endo, K., Okamoto, K., Fujimoto, E., and Ide, C. Extracellular matrix of human amnion manufactured into tubes as conduits for peripheral nerve regeneration. J Biomed Mater Res **63,** 591, 2002.
16. Mohammad, J., Shenaq, J., Rabinovsky, E., and Shenaq, S. Modulation of peripheral nerve regeneration: a tissue-engineering approach. The role of amnion tube nerve conduit

across a 1-centimeter nerve gap. Plast Reconstr Surg **105,** 660, 2000.
17. Niknejad, H., Peirovi, H., Jorjani, M., Ahmadiani, A., Ghanavi, J., and Seifalian, A.M. Properties of the amniotic membrane for potential use in tissue engineering. Eur Cell Mater **15,** 88, 2008.
18. Liliensiek, S.J., Nealey, P., and Murphy, C.J. Characterization of endothelial basement membrane nanotopography in rhesus macaque as a guide for vessel tissue engineering. Tissue Eng Part A **15,** 2643, 2009.
19. Szurman, P., Warga, M., Grisanti, S., Roters, S., Rohrbach, J.M., Aisenbrey, S., Kaczmarek, R.T., and Bartz-Schmidt, K.U. Sutureless amniotic membrane fixation using fibrin glue for ocular surface reconstruction in a rabbit model. Cornea **25,** 460, 2006.
20. Wilshaw, S.P., Kearney, J.N., Fisher, J., and Ingham, E. Production of an acellular amniotic membrane matrix for use in tissue engineering. Tissue Eng **12,** 2117, 2006.
21. Wilshaw, S.P., Kearney, J., Fisher, J., and Ingham, E. Biocompatibility and potential of acellular human amniotic membrane to support the attachment and proliferation of allogeneic cells. Tissue Eng Part A **14,** 463, 2008.
22. Hoemann, C.D., Sun, J., Chrzanowski, V., and Buschmann, M.D. A multivalent assay to detect glycosaminoglycan, protein, collagen, RNA, and DNA content in milligram samples of cartilage or hydrogel-based repair cartilage. Anal Biochem **300,** 1, 2002.
23. Farndale, R.W., Buttle, D.J., and Barrett, A.J. Improved quantitation and discrimination of sulphated glycosaminoglycans by use of dimethylmethylene blue. Biochimica et biophysica acta **883,** 173, 1986.
24. Liotta, L.A., Lee, C.W., and Morakis, D.J. New method for preparing large surfaces of intact human basement membrane for tumor invasion studies. Cancer Lett **11,** 141, 1980.
25. Chua, W.K., and Oyen, M.L. Do we know the strength of the chorioamnion? A critical review and analysis. Eur J Obstet Gynecol Reprod Biol **144 Suppl 1,** S128, 2009.
26. Roeder, R., Wolfe, J., Lianakis, N., Hinson, T., Geddes, L.A., and Obermiller, J. Compliance, elastic modulus, and burst pressure of small-intestine submucosa (SIS), small-diameter vascular grafts. J Biomed Mater Res **47,** 65, 1999.
27. Tosun, Z., Villegas-Montoya, C., and McFetridge, P.S. The influence of early-phase remodeling events on the biomechanical properties of engineered vascular tissues. J Vasc Surg **54,** 1451, 2011.
28. Duprey, A., Khanafer, K., Schlicht, M., Avril, S., Williams, D., and Berguer, R. *In vitro* characterisation of physiological and maximum elastic modulus of ascending thoracic aortic aneurysms using uniaxial tensile testing. Eur J Vasc Endovasc Surg **39,** 700, 2010.
29. Hennerbichler, S., Reichl, B., Pleiner, D., Gabriel, C., Eibl, J., and Redl, H. The influence of various storage conditions on cell viability in amniotic membrane. Cell Tissue Bank **8,** 1, 2007.
30. McFetridge, P.S., Abe, K., Horrocks, M., and Chaudhuri, J.B. Vascular tissue engineering: bioreactor design considerations for extended culture of primary human vascular smooth muscle cells. ASAIO J **53,** 623, 2007.
31. Iida, N., and Mitamura, Y. Role of physical properties of resistance vessel wall in regulating peripheral blood flow—II. Structural and mechanical behavior. J Biomech **22,** 119, 1989.
32. Iida, N. Physical properties of resistance vessel wall in peripheral blood flow regulation—I. Mathematical model. J Biomech **22,** 109, 1989.
33. Meller, D., Pires, R.T., Mack, R.J., Figueiredo, F., Heiligenhaus, A., Park, W.C., Prabhasawat, P., John, T., McLeod, S.D., Steuhl, K.P., and Tseng, S.C. Amniotic membrane transplantation for acute chemical or thermal burns. Ophthalmology **107,** 980; discussion 990, 2000.
34. Koizumi, N., Rigby, H., Fullwood, N.J., Kawasaki, S., Tanioka, H., Koizumi, K., Kociok, N., Joussen, A.M., and Kinoshita, S. Comparison of intact and denuded amniotic membrane as a substrate for cell-suspension culture of human limbal epithelial cells. Graefes Arch Clin Exp Ophthalmol **245,** 123, 2007.
35. Lim, L.S., Riau, A., Poh, R., Tan, D.T., Beuerman, R.W., and Mehta, J.S. Effect of dispase denudation on amniotic membrane. Mol Vis **15,** 1962, 2009.
36. Portmann-Lanz, C.B., Ochsenbein-Kolble, N., Marquardt, K., Luthi, U., Zisch, A., and Zimmermann, R. Manufacture of a cell-free amnion matrix scaffold that supports amnion cell outgrowth *in vitro*. Placenta **28,** 6, 2007.
37. Kurane, A., Simionescu, D.T., and Vyavahare, N.R. *In vivo* cellular repopulation of tubular elastin scaffolds mediated by basic fibroblast growth factor. Biomaterials **28,** 2830, 2007.
38. Yokota, Y., Taniguchi, R., Kawamura, Y., Nogata, F., Morita, H., Uno, Y., Sloten, J., Verdonck, P., Nyssen, M., Haueisen, J., and Magjarevic, R. Estimation of carotid stiffness using ultrasonic dynamic images for evaluating the degree of arteriosclerosis. In: Proceedings of the 4th European Conference of the International Federation for Medical and Biological Engineering. Berlin/Heidelberg: Springer, 2009, part 7, pp. 856–860.
39. Raitakari, O.T., Salo, P., and Ahotupa, M. Carotid artery compliance in users of plant stanol ester margarine. Eur J Clin Nutr **62,** 218, 2008.

Address correspondence to:
Peter McFetridge, Ph.D.
J. Crayton Pruitt Family Department of Biomedical Engineering
University of Florida
P.O. Box 116131
Gainesville, FL 32611–6131

E-mail: pmcfetridge@bme.ufl.edu

Received: February 24, 2012
Accepted: May 11, 2012
Online Publication Date: June 28, 2012